Crack control for repair and strengthening of reinforced concrete structures using the multi-cracking behaviour of Ultra-high Performance Fibre Reinforced Shotcrete (UHPFRSC)

Andre Strotmann[1,*], Jörg Jungwirth[1]

[1] Munich University of Applied Sciences (MUAS), Institute for Material and Building Research (IMB), Munich, Germany

Abstract. Ultra-High Performance Fibre Reinforced Concrete (UHPFRC) is an innovative material for the repair and/or strengthening of reinforced concrete structures. In the field of traffic infrastructure, the outstanding mechanical properties are used as a protective surface layer and to increase the load capacity of the structure. UHPFRC is characterised by a dense granular structure and correspondingly high resistance against chloride attack. The material is typically applied as cast in-situ concrete. To optimise implementation of the strengthening and repair method, the UHPFRC is applied as sprayed concrete, so-called Ultra-High Performance Fibre Reinforced Shotcrete (UHPFRSC). The research aims to increase the service life of damaged and/or overloaded structures. Crack widths in the UHPFRSC layer must be limited to avoid migration of chlorides. The thin UHPFRSC layer provides crack distribution and control of localised macro cracks in the existing reinforced concrete structure. The fibres in the Ultra-High Performance Shotcrete (UHPSC) allows for limiting the crack width to 50 µm. When the UHPFRSC is applied on cracked reinforced concrete, it can be assumed that multi-cracking in the UHPFRSC surface layer will provide a chloride-dense layer equivalent to a coating. Under load, the two layers - UHPFRC and RC - act as a composite. For structural analysis, a particular focus must be placed on the interaction between cementitious materials. In addition, the pre-damage and pre-loading of the existing structure will influence the structural behaviour and crack formation. The paper presents the results of bending tests of UHPFRC - RC composite elements. The investigation shows the outstanding crack control behaviour of UHPFRSC. Based on this investigation, an analytical model will be provided, and a calculation of the crack widths will be derived. The research presents a central aspect of a large interdisciplinary research project at Munich University of Applied Science, called i-SCUP.

1 State of the Art

Germany's traffic infrastructure (bridges, tunnels, parking decks, etc.), as well as the structures of the buildings are typically 30 to 80 years old. Many of these structures have been damaged because of chloride attack and excessive loads. Therefore, there is a high demand for efficient repair and strengthening concepts to ensure that structures conform to today's requirements.

UHPC's low porosity leads to high resistance to chemical and physical attacks [1]. These properties are highly suitable for strengthening and repair projects [2]. The issue of durability in a cracked UHPFRC layer is analogous to cracks in reinforced concrete. Chlorides penetrate cracked concrete or UHPFRC much faster than uncracked concrete. Penetration resistance to aggressive media decreases as the crack width increases [3].

The technology presented has a high potential for strengthening and repairing reinforced concrete structures. The Swiss guideline, SIA 2052, includes design approaches for strengthening with cast UHPFRC [4]. Structures have already been strengthened by using ultra-high performance materials, such as cast UHPFRC for the Viaduct de Chillon [5] or UHPFRSC for a tunnel strengthening manufactured by Lafarge Holcim, together with Freyssinet [6].

At Munich University of Applied Sciences, an extensive experimental program has been carried out regarding the material properties of UHPFRSC. A particular focus was on proving the pumpability and sprayability of the very dense material. Using specifically designed mixtures, UHPFRSC is a well-suited material for the shotcreting process. Application is possible with conventional high-performance construction machinery [7].

The specific high-performance material properties of classic UHPFRC could also be achieved using the spaying process for UHPFRSC [8]. However, there are significant differences depending on the direction of loading and spraying. The spraying process leads to an anisotropic effect caused by fibre orientation. The compression strength perpendicular to the spraying direction is between 120 MPa and 130 MPa, depending on whether cylinders or cubes have been tested. Compressive strength of up to 190 MPa was observed in the direction of

* Corresponding author: andre.strotmann@hm.edu

spraying, [8]. There is a direct correlation between fibre orientation and compressive strength [9]. The quasi-two-dimensional fibre orientation of the UHPFRSC thus produces a quasi-orthotropic behaviour in the material. The fibres also affect ductile material behaviour under compressive loading. The Young's modulus is 41.5 GPa on average and the tensile strength for hinged prismatic specimens is 6.0 MPa. Depending on the orientation of the specimen and the type of test, the flexural tensile strength is between 15.6 MPa to 23.5 MPa. The UHPFRSC shows strain-hardening behaviour under tensile loading. The strain-hardening effect results in a multi-crack formation, which is highly favourable for durability [8].

First investigations of the crack bridging effect of the UHPFRSC layer show remarkable results. The experimental investigations focus on the cracking behaviour of UHPFRSC-concrete composite elements under consideration of quasi-monolithic and specifically generated de-bonded composite joints. The investigations were carried out on UHPFRSC-concrete composite elements loaded in tension. The crack-bridging effect depends on the interaction in the composite joint between the UHPFRSC and normal strength concrete. Small crack widths were detected in the UHPFRSC layer. In addition to the difference in the composite joint behaviour, the effect of steel rebar reinforcement in the UHPFRSC layers was considered. Using steel rebars could limit crack widths in the overlay to 0.1mm [10].

In contrast, localised crack openings of single cracks have been detected in non-reinforced UHPFRSC layers for large strain. An additional positive effect is generated by using a specifically generated debonding zone. Due to the optimisation, the crack bridging effect is controllable. The considerations show that the additional UHPFRSC layer is suitable for repairing and strengthening reinforced concrete structures. Monolithic joint behaviour was detected in the investigations, but the joint always had to be kept under special observation [10].

2 Strengthening and Repair Concept

Conventional repair and strengthening methods are often associated with a significant intervention in the existing structure. This results in high costs and long down-time for the urgently required infrastructure. Ultra-High Performance Fibre Reinforced Shotcrete can be used as an optimised repair and strengthening method.

Fig. 1 shows the basic scenario of repaired and strengthened concrete structures under bending. In the case shown, the loading causes tensile forces in the UHPFRSC layer. The figure illustrates the general concept for repair and strengthening by using UHPFRSC. The high tensile strength of high-performance concrete allows for a significant increase of the load-bearing capacity of the UHPFRSC-concrete composite elements. This effect can be increased by using rebars in the UHPFRSC layer.

The added UHPFRSC layer could prevent a local chloride penetration along a macro-crack in the reinforced concrete element. The cracks are sealed, preventing further penetration from chlorides. The small crack widths and the multi-crack formation in the UHPFRSC ensure the protection of the reinforced concrete below.

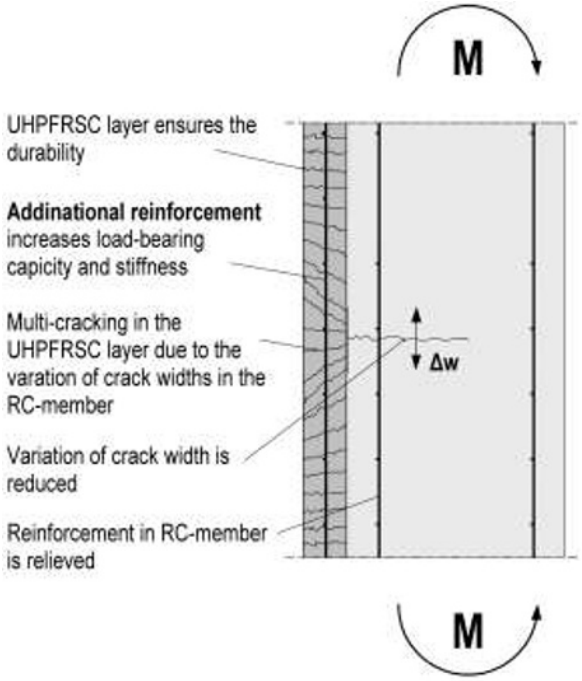

Fig. 1 Basic scenario of a damaged concrete structure under bending with repair and strengthening using UHPFRSC (adapted from [11])

Short steel fibres can achieve a crack-distributing effect similar to the conventional crack-distributing due to steel rebar in classical concrete structures. The crack-crossing steel fibres have a higher strength than the surrounding concrete matrix. Due to this, the crack will not continue to open, but secondary crack formation develops next to the initial crack (comparable to the crack-distributing effect in normal strength concrete). The spacing of this multi-cracking is only a few millimetres and the crack widths is very small. The measured crack opening is about 0.02 mm, compared to 0.2 mm for reinforced concrete [12].

The dense microstructure of the UHPFRC in an uncracked state provides remarkable protection against chloride penetration [13]. Fundamental studies have assumed from this protection that the mean strain in the UHPFRC does not exceed 1 ‰ (Charron et al. 2007) [2]. Further investigations on the transport properties regarding cracked concrete, e.g. [14], show that crack widths with a critical value do not have a noticeable influence on the transport processes.

It can be assumed that a macro-crack in the existing concrete is distributed under bending into many small cracks with small crack widths in the UHPFRSC layer. This effect is comparable to the results of the investigation regarding the crack formation of UHPFRSC-concrete composite elements under pure tension. An optional approach is to apply a debonding layer to achieve wider distributed cracking [10].

In addition to the local chloride penetration in cracks, the distributed chloride exposure on the surface must also be

considered. Two approaches regarding the repair and strengthening method are addressed: The first approach is to remove the chloride-loaded concrete and reprofile with UHPFRSC. The second is to leave the chloride-loaded concrete in the structure and seal it with UHPFRSC. This approach is efficient as it eliminates one work step on site. The feasibility of the respective alternatives depends on the degree of chloride loading, as well as the corrosion level of the reinforcement. The electrolyte resistance of the composite element also increases due to the application of UHPFRSC. This reduces the corrosion process to an expected harmless level. The lifetime of the repaired and strengthened concrete structure can be extended or recovered to its original state.

Strengthening the compression zone of concrete structures is also possible using a UHPFRSC layer. Due to the high compressive strength of UHPFRSC, efficient strengthening in the compression zone without a significant increase in self-weight is possible [10]. This case of repair and strengthening is not focused on in this paper.

3 Experimental Investigation

3.1. Area of Interest

The experimental investigation focuses on the area in the interface of the macro crack in the reinforced concrete in the UHPFRSC layer. The area is called Area of Interest in this paper.

A well-distributed crack pattern is essential for the application of the repair and strengthening concept with UHPFRSC. The macro-crack in the reinforced concrete that must be bridged should be distributed into several multi-cracks in the UHPFRSC with small crack openings. There is a point where the multi-cracks in the UHPFRSC layer come together in a small section at the tip of the crack in the reinforced concrete, as shown in Fig. 2a.

In addition to the crack formation described earlier, an alternative design of the composite joint can be used for an optimised crack pattern in the UHPFRSC layer. This approach is based on the method for crack-bridging with textile concrete. As shown in Fig. 2b, a debonding zone between UHPFRSC and normal concrete can be applied for optimised crack formation in the overlay. This debonding zone causes a free expansion length of the UHPFRSC layer under tensile load. An excellent distribution of the large local crack widths to several multi-cracks over a defined length in the overlayer is achieved [15]. Cracks will become oriented orthogonally to the normal-strength concrete surface and crack widths are very small.

The crack distribution behaviour in the UHPFRSC layer is investigated for both concepts as shown in Fig. 2. Special focus is on the interface between the UHPFRSC layer and the substrate with and without a debonding zone. The crack-bridging behaviour of UHPFRSC is evaluated with and without rebars in the UHPFRSC layer.

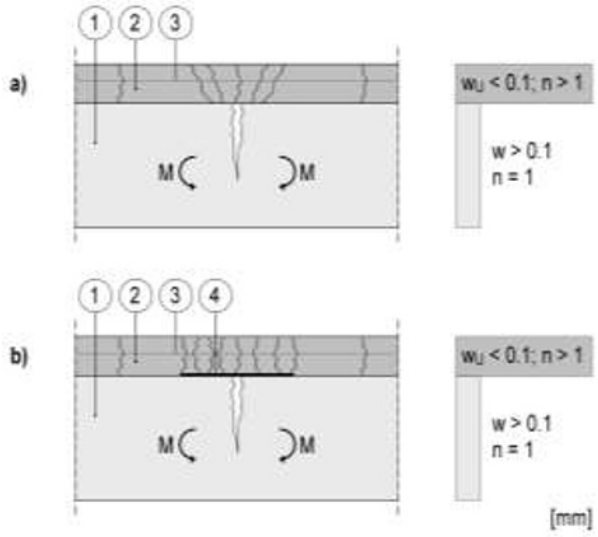

Fig. 2 Crack patterns in the overlay depending on the joint type ①NSC, ②UHPFRSC, ③Reinforcement, ④Debonding a) Composite member without debonding in the composite joint b) Composite member with debonding in the composite joint

3.2. Test Campaign

The test campaign of the UHPFRSC-concrete composite elements was performed using 4-point bending tests. Eight different configurations of the specimen were manufactured and tested. The beams (RC base beams) are 150 mm wide, 1180 mm long and 140 mm high reinforced concrete beams with a reinforcement of 2 x Ø8 mm rebars at the top and bottom. The length of the steel bars is 1200 mm, thus, they protrude 10 mm from the concrete body on each side. Furthermore, a shear reinforcement, as well as a reinforcement of the composite joint, has been placed using Ø8mm stirrups. The span between the bearings is 1050mm with a 65mm cantilever on each side. Load application is at one-third of the span. The UHPFRSC layer is an ultra-high strength, fibre-reinforced shotcrete from Lafarge Holcim with the product name Ductal® Grey Shotcrete. The UHPFRSC layer is applied on the surface of the RC base beam with a thickness of 40 mm. Half of the specimens are in also reinforced with additional rebars 2 x Ø6mm in the UHPFRSC layer. All different configurations of the specimens are shown in Fig. 3.

The specimens are named based on the following index:

Ux – RCy – Sz – No.

U: UHPFRSC	RC: Reinforced Concrete	S: Surface (NSC-RC)
x: Reinforcement	y: Notch	z: Surface preparation
a: non-reinforced b: reinforced	a: non-notched b: notched	a: bonded b: de-bonded
No. Specimen Number		

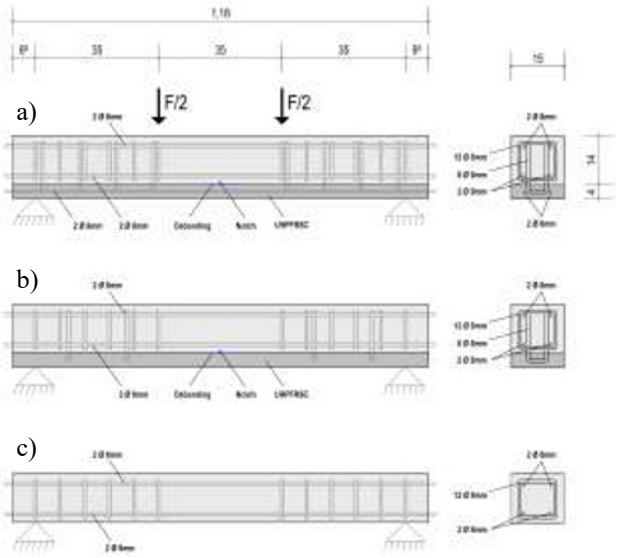

Fig. 3 Test setup and geometry of specimens a) Ub-RCa-Sa-No., b) Ua-RCa-Sa-No. c) Ref-1/2/3

The UHPFRSC-concrete composite beams are produced in spray boxes, as shown in Fig. 4. The spray boxes consist of two levels: there is the base level with the already-hardened NSC and the second level of UHPFRSC, which is applied on the surfaces of the reinforced concrete. To apply the UHPFRSC in the second level, conventional wooden framework is used. The NSC of the RC base beam is 32-34 days old on the day of spraying. The dimensions of the UHPFRSC layers are 1180x680mm, and the core in reinforced concrete is 1180x600mm. The different dimensions result from an overlap that is required for the sprayed layer. The spraying process leads to imperfections in the UHPFRSC at the edge of the formwork. The overlap is cut off before testing. Half of the RC base beams have a 0.5mm wide notch. As seen in Fig**.** 3, debonding zones in the composite joint were created by using coating material, which is polymer-bonded.

Fig. 4 illustrates the preparation of the surface of the base beams in a spray box. Four specimens in each spray box are placed next to each other. The procedure corresponds to the conventional repair methods. A rough joint was prepared with the HWJ. To ensure a good bond between NSC and UHPFRSC, the surface has been watered for around 12h before the application of the UHPFRSC. The specimens were treated directly after spraying with a conventional curing agent containing paraffin. The protection from drying close to the surface was prevented with a PE foil. The post-treatment is important to reduce load-independent stresses on the specimen. After spaying, the specimens are cut into the final form. Until testing, the specimens with the added UHPFRSC layer are stored at a constant temperature and humidity for 56-58 days.

The investigations of the material were carried out, providing the material properties under uniaxial loading for the evaluation of the results.

Fig. 4 Spray box with roughened NSC surface and watering of the surface before adding the UHPFRSC layer

3.3. Test Results

3.3.1 Strengthening

Besides the durability aspect in retrofitting, the strengthening aspect is a central point as to why UHPFRSC was used for this application. The load-deflection curves show the increase of the load-bearing capacity (Fig. 5). The force is the load applied by the hydraulic cylinder, which was logged by the control system of the testing machine. Deformations were measured at mid span by LVDT as deflection of the specimen. In addition, the central part of the test specimen with pure bending has been investigated using a 2D-DIC system. The data from the DIC system has been used to illustrate the vertical deformations in the following. By comparing the applied force, the increase of the load-bearing capacity due to the UHPFRSC layer (with and without additional rebars) can be described.

Fig. 5a shows the load-deflection curve of the specimens with a UHPFRSC layer, including an additional steel rebar reinforcement (Ub-RCa-Sa-1/2/3). The force is shown on the ordinate of the graph, and the vertical deformations in the middle of the specimen are shown on the abscissa. The configuration of the specimens does not contain any joint imperfection or a notch. Forces up to about 110 kN could be achieved. The vertical deformation of the beam at the maximum load is around 5 to 7 mm.

Fig. 5b is the equal representation of a load-deflection diagram as shown above. The load-deflection curves of specimens Ua-RCa-Sa-1/2/3 are shown. The specimens are the composite members without additional rebars in the UHPFRSC layer. The forces are 65 to 90 kN at about 3.5 to 5 mm deformation. Specimen Ua-RCa-Sa-3 shows an anomaly, as significantly higher forces were achieved in comparison to the other tests. The other specimens tested were in the range of about 60 kN. The increased load-bearing capacity of specimen Ua-RCa-Sa-3 may be the result of an ideal fibre distribution in the reinforcement layer, but this could not be proven conclusively. The fibre orientation is assumed to be random and quasi-parallel to the sprayed surface. With the distribution, a concentrated orientation of the fibres can

occur in the load direction, which has a positive effect on the load-bearing capacity.

Finally, in Fig. 5c, the three reference specimens are shown. The results are also shown in the load-deflection diagram under the same boundary conditions as above. The reference specimens Ref 1/2/3 are the base RC beams without the additional layer. The maximum force of the members is at around 42 kN with a vertical deformation of around 16 mm.

The comparison of the load-deflection curves of the reinforced specimens with those of the reference specimens shows a significant increase in the load-bearing capacity due to the additional layer.

The specimens Ub-RCa-Sa-1/2/3 were able to bear 110 kN, an increase in load-bearing capacity of more than 100 per cent compared with the reference specimens.

Specimen Ua-RCa-Sa-1/2/3 shows a load capacity increase of about 50 per cent due to the applied UHPFRSC layer without additional steel rebar reinforcement, not considering specimen Ua-RCa-Sa-3 due to its unusual higher load-bearing capacity.

It could be observed that for strengthened specimens, the deformations at the mid span at maximum load is significantly smaller than those of the reference specimens. It can be concluded that there is an increase in stiffness due to the lower deformations at higher loads compared to the reference.

In addition, it can be observed that the maximum values of the force applied, as well as the corresponding deformations, show a significantly wider spread in the case of the strengthened specimens. A simple comparison can be made with the reference specimens showing a minimal spread. It is assumed that the fibre distribution and orientation cause the wider spread as the fibre-reinforced high-performance concrete is a highly inhomogeneous material.

It can be concluded that the intended increase in load-bearing capacity and stiffness was achieved using a UHPFRSC layer.

3.3.2 Crack control

To investigate cracking, the central section of the composite beam was equipped with a 2D-DIC measuring system. The area of investigation was 35cm between the applied loads, and the height of the investigation area was 18cm, 14cm NSC, plus 4cm UHPFRSC. Post-testing, the DIC recordings were evaluated at all load levels. The main deformations were assessed in plane based on the two-dimensional deformation associated via the picture row sequence. The strain scaling was set to +/-0.75 to visualise the cracks.

In addition, horizontal sections were placed in relevant areas. The sections were arranged across the entire length of the area investigated. In total, three sections were generated. Two sections were placed in the RC base beam, at the level of the rebars. Furthermore, one section was placed in the middle of the UHPFRSC layer. The sections indicate the displacements in x-direction. The displacement in x-direction is given for each increment of the section. The increments start at the left edge with the

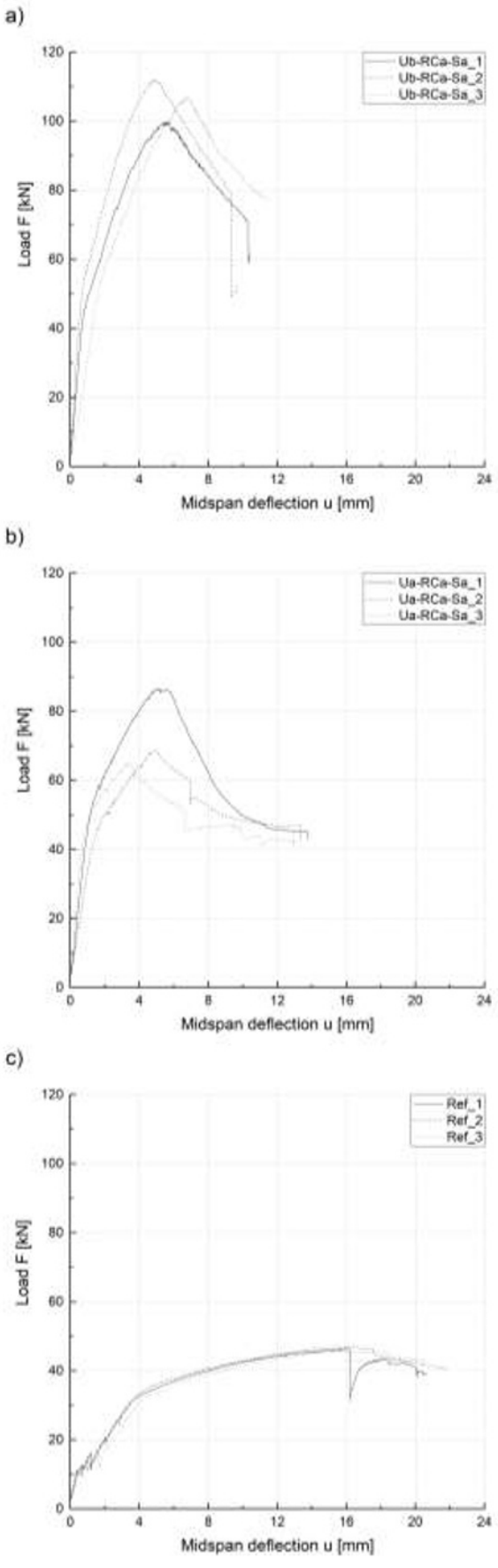

Fig. 5 Load-deflection curves of the tested specimens a) Ub-RCa-Sa-1/2/3 b) Ua-RCa-Sa-1/2/3, c) Ref-1/2/3

value of zero. The end of the analysed area is 350mm at the right edge. The distance from the left edge is shown in mm on the ordinate. The length of each increment depends on the evaluation of the DIC measurement. The corresponding displacements are shown on the abscissa. The method of analysis allows for the visualisation of cracks. Discontinuities on the curve represent cracks, whereas the step height indicates the crack width. This type of illustration enables the comparison of a large number of cracks.

The analysis of the tests described above are combined in Fig. 6a) regarding crack formation and crack bridging. The diagram shows specimen Ub-RCa-Sa-1 with a rebar in the UHPFRSC layer. Crack spacing and opening is shown in the diagram on the bottom via the main deformations and the crack pattern is indicated in red in the picture on top. The presented load level is the ultimate limit state just before failure. The dashed line indicates the joint between NSC and UHPFRSC. In Fig. 6a), nine cracks can be observed in the reinforced concrete. A significantly higher number of cracks can be observed in the UHPFRSC layer. The three previously described sections are indicated with coloured lines (black, red, blue) in the crack pattern. The deformation in x-direction is shown in the diagram below. The three curves show the horizontal deformation. The grey arrows are the reference crack pattern and the discontinuity of the deformation (crack opening). The line refers to a point on the section in the crack pattern and shows the curve of the deformations in the corresponding diagram. For each crack, one discontinuity can be identified. The discontinuity steps can be quantified to a crack width of 0.10mm and larger. A significantly higher number of discontinuity steps equivalent to the number of cracks can be observed in the deformation curve of the UHPFRSC, as well as in the crack pattern. The corresponding crack widths are smaller than in the reinforced concrete by about a power of ten. This effect can be called crack bridging. For each wide-open crack in the reinforced concrete, multi-cracks occur in the UHPFRSC.

Fig. 6b shows the result of composite beam Ua-RCa-Sa-3 without additional rebar. The specimen shows the same crack formation and bridging effect as described above. The crack pattern and the diagram data logged were the ultimate limit state just before failure. The correlation between the crack pattern and the diagram can also be seen in the case of specimen Ub-RCa-Sa-1, marked by the grey arrow lines. In the composite specimen, five cracks were detected in the reinforced concrete. In the UHPFRSC layer, significantly more cracks can be observed. Crack widths of 0.10mm and larger can be noted from the corresponding deformation curve in the diagram. A large number of discontinuity steps can be detected in the UHPFRSC, which fit the associated crack pattern. It can be concluded that crack bridging has occurred in the UHPFRSC. However, the crack widths are up to 0.10mm or larger.

The analysis of the crack widths takes into account that the specimens are loaded in bending and that the cracks occur on different levels with different lever arms. Thus, larger deformations and larger strains result in the UHPFRSC layer. The presented crack widths correlate to

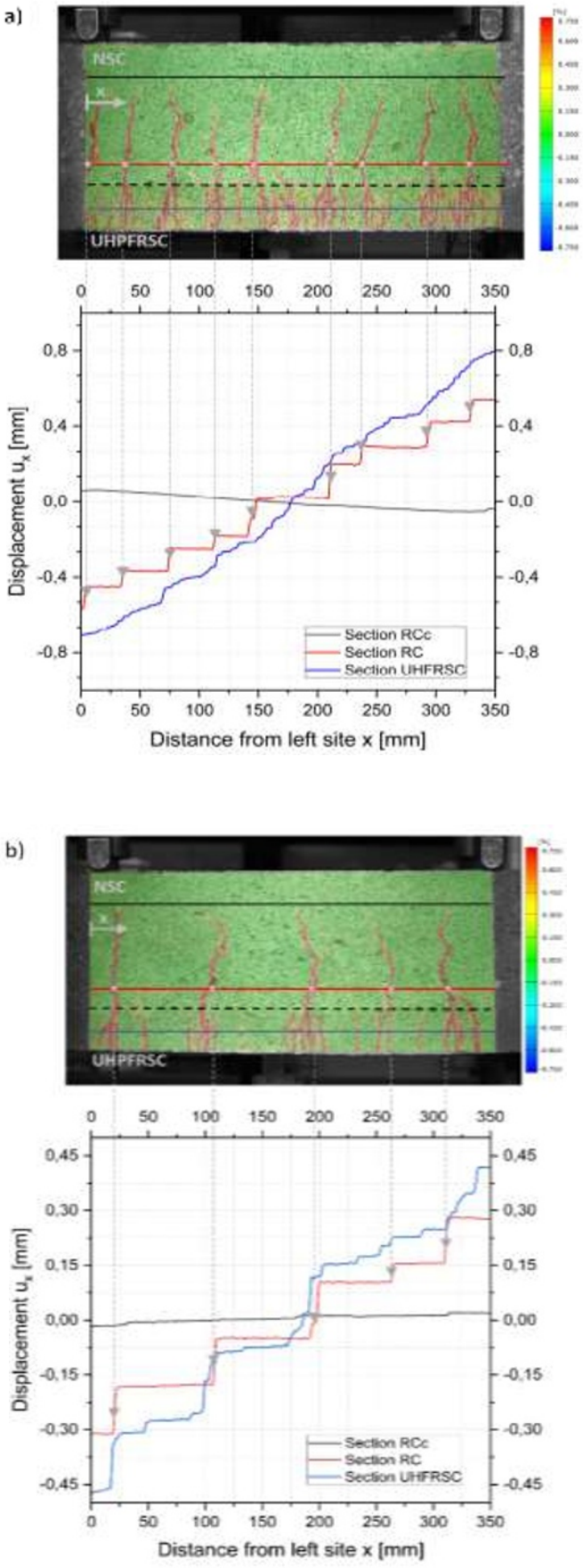

Fig. 6 Crack pattern using DIC system by means of the main deformations and the x deformations in sections over the height of the composite element at load F_{max} a) Ub-RCa-Sa-1 b) Ua-RCa-Sa-3

the strains. The strain state of the layers considered is shown in Fig. 7.

No systematic joint failure can be detected in the crack pattern in Fig. 6. This conclusion can be drawn because no strains can be observed in the joint. Therefore, a monolithic joint behaviour can be assumed.

The comparison of specimens Ub-RCa-Sa-1 and Ua-RCa-Sa-3 shows a clear influence of the steel reinforcement bar on the crack bridging. The use of rebars in the UHPFRSC layer results in a significantly finer crack pattern. In addition, there is a more homogeneous crack distribution with more stable crack widths in the Ub-RCa-Sa-1 specimen than in the specimen without rebars. In contrast, Ua-RCa-Sa-3 shows breakthrough cracks from the NSC into the UHPFRSC. In Fig. 6b, the cracks in the NSC and UHPFRSC are clearly superimposed featuring a crack width of more than 0.10mm. It is essential to consider the influence of bending is in this case, though the breakthrough of the crack can clearly be seen. Generally, it can be concluded that crack bridging in the UHPFRSC is possible with and without additional steel reinforcement. Thus, crack control for repair and strengthening of reinforced concrete structures is feasible with a UHPFRSC overlay.

In addition, it has to be pointed out that not only were an increased number of cracks produced in the UHPFRSC, but additional cracks were also formed in the reinforced concrete by the overlay. In specimen Ua, five cracks can be detected in the reinforced concrete, and in specimen Ub, nine cracks can be detected. Compared to the reference specimens, the increase of cracks in the reinforced concrete gets even clearer. In the reference specimens, only three cracks can be detected in the area of investigation. The additional cracking in the reinforced concrete is a positive aspect regarding the durability as well as the load-bearing capacity. A reduced crack opening in the reinforced concrete increases the durability due to greater resistance to aggressive agents. In addition, the reduced crack spacing and reduced crack opening leads to a higher tension stiffening effect and provides a stiffer structure and, as a result, better behaviour in service ability limit state (SLS).

4 Conclusion and Outlook

The specimens Ub-RCa-Sa-1/2/3 strengthened with UHPFRSC and rebars were able to carry 110 kN, an increase in load-bearing capacity of more than 100 per cent compared with the reference specimens.

Specimens Ua-RCa-Sa-1/2/3 (UHPFRSC layer without additional steel rebar) showed an increase in load capacity of about 50 per cent, whereby specimen Ua-RCa-Sa-3 is not considered due to its unusual higher load-bearing capacity.

It has been observed for the strengthened specimens that the deformations at mid span for ultimate load are significantly less than those of the reference specimens. It can be concluded that there is an increase in stiffness due to the UHPFRSC layer compared to the reference.

In addition, it can be observed that the maximum values of the force applied, as well as the corresponding deformations, are significantly more spread out in the case of the strengthened specimens. A comparison can be carried out with the reference specimens, which show a minimal spread. It can be assumed that the fibre distribution and orientation cause the spread because the fibre-reinforced high-performance concrete is a highly inhomogeneous material. Overall, the intended increase in load-bearing capacity and stiffness was demonstrated.

Comparing the specimens Ub-RCa-Sa-1 and Ua-RCa-Sa-3 shows a clear influence of the steel reinforcement on the crack formation. Using steel reinforcement bars in the UHPFRSC results in a significantly finer crack pattern. In addition, more homogeneous crack distribution with more stable crack widths can be observed with specimen Ub-RCa-Sa-1 compared to specimen without additional steel bars. Specimen Ua-RCa-Sa-3 shows breakthrough cracks from the NSC into the UHPFRSC. The influence of the lever arm in bending is an important consideration in this case, but the is a strong affinity to breakthrough cracks.

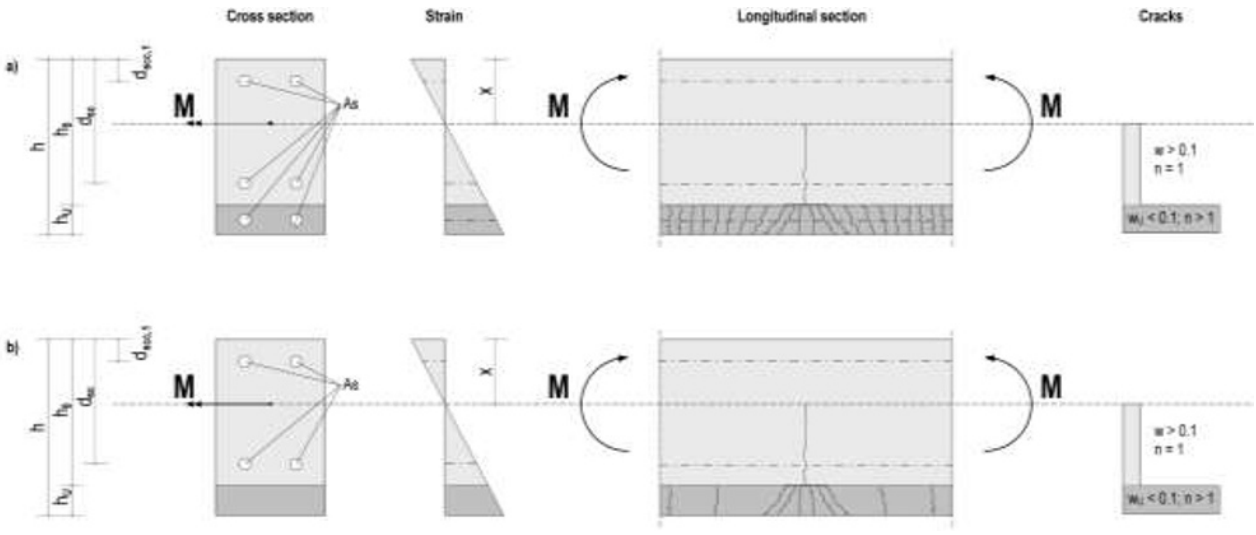

Fig. 7 Strain distribution over the cross-section and longitudinal cracking of the composite member a) specimen with additional steel rebar reinforcement in UHPFRSC, b) specimen without additional steel rebar reinforcement in UHPFRSC

The investigation shows that the UHPFRSC layer provides the intended crack bridging effect and suitable crack control.
Regarding the crack widths, it must be considered that the specimens were tested in bending, and the considered crack widths were determined with different lever arms. Hence, larger deformations and thus larger strains result in the UHPFRSC layer. The crack widths shown are correlated with the strains.
It should also be noted that an increased number of cracks was produced in the UHPFRSC layer and additional cracks were induced in the reinforced concrete. In specimen Ua, five cracks can be detected in the reinforced concrete and in specimen Ub, nine cracks can be detected. The increase in the number of cracks in the reinforced concrete is even more significant in comparison to the reference specimens, where only three cracks can be observed.
No systematic joint failures are detected. Thus, a monolithic behaviour could be assumed for the joint between UHPFRSC and NSC. However, the joint should always be kept under special observation.
As part of the research project, the time-dependent material behaviour and resulting constraining stresses with influence on crack formation will be investigated in further studies. Furthermore, additional test campaigns on crack formation on bending beams with various configurations are carried out in the following.
The goal of the ongoing investigations is to determine and recommend the limit of application for each configuration, depending on the variation of the crack width. Different ranges of crack width and the associated crack control system require an appropriate design approach. Structural analysis models for the design approaches will be developed using FE simulations. The corresponding maximum crack widths regarding the chloride tightness, as well as the reduction of the corrosion level, will be defined by cooperative material technology investigations.

Acknowledgements

The authors would like to thank the German Federal Ministry of Education and Research for funding the project "Repair and strengthening of reinforced concrete structures using thin UHPFRSC layers: Fields of application, design, durability, processing technology" (grant number 13FH676IX6) within the research programme "Research at Universities of Applied Sciences". We would also like to thank our industrial partners Karrié Bauwerkserhaltung GmbH and LafargeHolcim Ltd. (Jona, Switzerland). Furthermore, we would like to thank the entire research team involved in the i-SCUP project, in particular the leading Professors Prof. Dr.-Ing. Andrea Kustermann, Prof. Dr.-Ing. Christoph Dauberschmidt, as well as the Research Assistant M.Eng. Toni Pollner for their cooperation.

References

1. E. Fehling, M. Schmidt, T. Teichmann, K. Bunje, R. Bornemann, and B. Middendorf, *Schriftenreihe Baustoffe und Massivbau*, Heft 1: *Entwicklung, Dauerhaftigkeit und Berechnung ultrahochfester Betone (UHPC): Forschungsbericht DFG FE 497/1-1* (Kassel Univ. Press, Kassel, 2005) [ger].
2. J.-P. Charron, E. Denarié, and E. Brühwiler, Mater Struct **40**, 3 (2007).
3. B. Savija: *Experimental und numerical investigation of chloride ingress into cracked concrete* (Delft, 2014).
4. SIA, *Ultra-Hochleistungs-Faserbeton: Baustoffe, Bemessung und Ausführung* (Schweizerischer Ingenieur und Architektenverein, Zürich, Schweiz, 2016), SIA 2052.
5. H. Sadouki, E. Brühwiler, and D. Zwicky, in *Concrete Repair, Rehabilitation and Retrofitting IV*, Ed. by F. Dehn, H.-D. Beushausen, M. Alexander, and P. Moyo, 122–123 (CRC Press, 2015).
6. A. Huynh, B. Petit, F. Teply, A. Autissier, and C. Larive, in *Proceedings / RILEM*, PRO 106: *Proceedings of the AFGC-ACI-fib-RILEM International Conference on Ultra-High Performance Fibre-Reinforced Concrete, 2-4 October 2017, Montpellier, France*: *UHPFRC 2017 Designing and building with UHPFRC: New large-scale implementations, recent technical advances, experience and standards*, Ed. by F. Toutlemonde and J. Resplendino, 717–724 (RILEM publications, Bagneux, 2017).
7. J. Jungwirth, A. Kustermann, C. Dauberschmidt, T. Pollner, and A. Strotmann, in *fib Proceedings*, No. 51: *Concrete Structures for Resilient Society*: *Proceedings of the fib Symposium 2020*, Ed. by B. Zhao and X. Lu, 7–15 (2020).
8. A. Strotmann, T. Pollner, A. Kustermann, and J. Jungwirth, in *Spritzbeton-Tagung 2021*, Ed. by R. Galler, G. Goger, and W. Kusterle, 201–220 (2021).
9. P. Riedel and T. Leutbecher, Beton- und Stahlbetonbau **115**, 10 (2020).
10. A. Strotmann and J. Jungwirth, in *fib Symposium 2021, Concrete Structures: New Trends for Eco-Efficiency and Performance, fib Symposium 2021 from 14 to 16 June 2021 in Lisbon, Portugal* .
11. J. Jungwirth, A. Kustermann, C. Dauberschmidt, A. Strotmann, T. Pollner, and M. Schmidt, in *Proceedings of HiPerMat 2020*: *5th International Symposium on Ultra-High Performance Concrete and High Performance Materials*, Ed. by E. Fehling and B. Middendorf, 173–174 (2020).
12. J. Jungwirth: *Zum Tragverhalten von zugbeanspruchten Bauteilen aus Ultra-Hochleistungs-Faserbeton* (Lausanne, 2006).
13. J. Provete Vincler, T. Sanchez, V. Turgeon, D. Conciatori, and L. Sorelli, Cement and Concrete Research **117** (2019).
14. Z. Ma, T. Zhao, and X. Yao, ACT **14**, 12 (2016).
15. C. Morales Cruz and M. Raupach, MATEC Web Conf. **289**, 6 (2019).